Int J Mech Mater Des (2022) 18:461–473
https://doi.org/10.1007/s10999-021-09573-7

Fluid structure interaction simulation of thermal striping in a t-junction pipe made of functionally graded material

Ziyi Su · Kazuaki Inaba · Amit Karmakar · Apurba Das

Received: 18 May 2021 / Accepted: 7 October 2021 / Published online: 22 October 2021

Abstract In a nuclear power plant, thermal striping occurs at the T-junction, where high-temperature steam and low-temperature processed fluids mix. The non-uniform temperature distribution and temperature fluctuation in the pipe produced by thermal striping may lead to cracks and high cycle thermal fatigue failure. The use of a thermal sleeve can prevent this issue to a certain extent, but delamination is a major concern in such thermal striping. Functionally graded materials (FGMs) in which the material properties are graded along the thickness direction can relieve the thermal stress gradient in the pipe, eliminating the delamination problem. In this study, a one-way fluid structure interaction simulation of ceramic and structural steel functionally graded T pipes under thermal striping was performed using the detached eddy simulation method. The initial condition of velocity and temperature was used based on the "WATLON" experiment conducted by the Japan Atomic Energy Agency. Spectral analysis was performed to evaluate the temperature fields for both the fluid and the pipe, as well as to determine the temperature fluctuation characteristic. The temperature variation in the pipe was then used in the transient structural analysis to evaluate fluctuations in the thermal stress. Finally, the rainflow counting method was employed to determine the stress cycles of the pipe. The thermal stress cycles of homogenous, composite, and FGM pipes were compared. The reduced amplitude of the stress cycle of the FGM pipe confirms a higher fatigue life and potential application of the FGM at the T-junction.

Keywords Functionally graded material · T junction pipe · Detached eddy simulation · Thermal striping · Thermal stress

Z. Su (✉) · K. Inaba
Department of Mechanical Engineering, Tokyo Institute of Technology, 2-12-1 Ookayama, Meguro, Tokyo 152-8550, Japan
e-mail: su.z.aa@m.titech.ac.jp

A. Karmakar
Department of Mechanical Engineering, Jadavpur University, 188 Raja S. C. Mullik Road, Kolkata 700032, India

A. Das
Department of Aerospace Engineering and Applied Mechanics, Indian Institute of Engineering Science and Technology, Botanical Garden Rd, Howrah 711103, India

1 Introduction

Thermal striping occurs when fluids with different temperatures mix. Temperature variation generated by the thermal striping may lead to cracks and thermal fatigue failure in the structure. In 1998, a leakage was reported at the nuclear power plant (NPP) in Civaux, France (Chadeyron 1999). Investigations (Blondet and

Faidy 2002; Chapuliot et al. 2005) reported a through-wall crack downstream of a T junction, where hot and cold streams mixed. Moreover, several studies have also been conducted to better understand thermal striping. Kawamura et al. (2003) conducted thermal striping tests in a mixing T junction with a velocity ratio ranging from 0.1 to 5 and a temperature gradient of 40 °C to characterize the flow patterns and temperature fluctuation in the thermal striping. Japan Atomic Energy Agency performed a water experiment called "WATLON" to clarify the thermal hydraulic aspects of thermal striping with a T pipe (Kamide et al. 2009). Miyoshi et al. (2013) determined the temperature characteristics at the pipe inner surface to figure out the thermal fatigue in T pipe. Chuang and Ferng (2017) also conducted the experiment to reveal the thermal striping characteristics in a T pipe. Recently, Zhou et al. (2019a, b) reported the mixing characteristics at the T junction which was horizontal oriented. In addition to experimental studies, numerical studies on thermal striping have also been conducted by many researchers owing to the development of computational fluid dynamics. The Reynolds averaged Navier–Stokes model is not suitable to describe the realistic mixing of flow in thermal striping (Nakamura 2007; Höhne 2014). However, the large eddy simulation model (Jayaraju et al. 2010; Ayhan and Sökmen 2012; Timperi 2014; Selvam et al. 2015) and detached eddy simulation model (Nakamura et al. 2009; Kang et al. 2019) can adequately capture the characteristics of thermal striping. For evaluating the thermal fatigue in T pipe, Tanaka et al. (2010) numerically studied the thermal striping with proposed evaluation method. Recently, Evrim and Laurien (2021) numerically studied the thermal mixing mechanisms at T junctions, where a wall-resolved large eddy simulation was used.

The non-uniform temperature distribution in the structure causes thermal fatigue and cracking. Thermal sleeves can prevent the transfer of temperature fluctuations. However, delamination is a major problem when using such thermal sleeves. Functionally graded material (FGM) is a constituent of two materials that are graded along the thickness direction and has the potential to relieve the thermal stress gradient in a pipe. Hence, the use of FGM in T-junction pipes can overcome this delamination problem. The concept of FGM was first introduced by Kawasaki and Watanabe (1997) in 1984 for the development of thermal barrier materials. In FGM, the compositions would continuously change from one phase to another and as smoothly as the designed gradient. This smooth interface in the material reduces the stress concentration, and de-bonding or delamination can be eliminated. Applications of FGMs in aviation, energy, nuclear power plants, and medical fields have increased exponentially over the last decade (Saleh et al. 2020). For the pipe application, FG pipe had been fabricated by the centrifugal force method and the micro structure was investigated. (Watanabe et al. 2005). Thermal striping in the T-junction pipe is an unavoidable situation, and the application of FGM can mitigate the thermal stress by reducing the fluctuation of temperature from the fluid to the pipe.

From the review of open literature, it is evident that thermal striping is a concern for T-junction pipes in NPP. Several experimental and analytical works have been reported on the wall temperature and fatigue life of pipes. However, the use of FGM in T-junction pipes for potentially reducing thermal striping and enhancing fatigue life has not received much attention; further, analysis of thermal stripping in FGM T-junction pipes is rare. Therefore, to fill the apparent void in research identified in the literature review, this study simulated the performance of structural steel and ceramic functionally graded T pipes under thermal striping using a one-way fluid structure interaction simulation using the detached eddy simulation method. The main and branch flow condition of velocity and temperature in the simulated thermal striping case is the same as in the "WATLON" experiment conducted by the Japan Atomic Energy Agency (Kamide et al. 2009). Spectral analysis was performed to evaluate the temperature field in both the fluid and the pipe. The temperature field was obtained from the DES simulation and was used to classify the temperature fluctuation characteristics. Finally, the temperature field in the pipe was imported into the transient structural analysis to evaluate the fluctuation of the thermal stress. The rainflow counting method was used to count the stress cycles during the calculated duration. The amplitudes of the stress cycle and mean stress of the junction pipes made of homogenous, composite, and FGM were compared.

2 Numerical simulation

2.1 Simulation model

The geometry of the T-junction pipe and the flow conditions used in the simulation are referred to in the WATLON experiment. Figure 1 shows the schematic diagram of the calculation domain. The main pipe has 150 mm in diameter (D_m) and 7.6 mm in thickness (t_m). The branch pipe has 50 mm in diameter (D_b) and 5.3 mm in thickness (t_b). Table 1 lists the flow conditions of the main and branch pipes. The value of the momentum ratio (M_R), calculated using the equation $M_R = \frac{4D_m V_m^2}{\pi D_b V_b^2}$, is larger than 1.35. This indicates that the flow pattern is wall jet flow. According to the research conducted by Kamide et al. (2009), the stratified flow of thermal striping has the largest potential for generating thermal fatigue in the pipe owing to a higher fluctuation of temperature.

2.2 Thermal striping simulation set up

The mesh of the simulation model was generated using ICEM CFD. Figure 2 shows the mesh at the cross-section of the main pipe and the side view of T-junction. Hexahedral elements were used for mesh generation. In the fluid domain, the first layer at the boundary has a height of $1.2\text{x}10^{-5}$ m. In the solid domain, the hexahedral mesh elements have the same thicknesses of $2.4\text{x}10^{-4}$ m and $1.7\text{x}10^{-4}$ m in the main and branch pipes, respectively to accurately capture temperature and stress fluctuation in the thickness direction. There are a total of 2.1 million nodes in the computational domain (fluid domain ≈ 1.2 million nodes; solid domain ≈ 0.9 million nodes).

Table 1 Flow conditions in the main and branch pipes

	Main	Branch
Temperature [°C]	48	33
Mean velocity [m/s]	1.46	1.0

The components of the FG T pipe were considered to be structural steel and ceramic. The material gradually changed from ceramic to structural steel from the inner side of the pipe to the outer side. Su et al. (2021) used a multi-layer model to simulate FGM in the commercial FEM software. The transient heat conduction simulation of FG pipe, which related to the conjugate heat transfer in the one-way fluid structure interaction simulation in this work was validated when 8 or more layers used in multi-layer model. Therefore, in the present work, the mesh of the FGM solid domain is divided into 8 layers, and each layer is assigned the material property based on the power-law distribution (Das and Karmakar 2018), as given in Eq. (1).

$$P(Z) = (P_1 - P_2)\left(\frac{(Z-1)}{8} + \frac{1}{16}\right)^N + P_2, Z = 1, 2, 3, \ldots, 8 \quad (1)$$

where N is the power law index. By changing the value of the index, the material gradient in the thickness direction can be tailored based on the application. Three types of gradient indexes, 0.2, 1, and 5 were used corresponding to Case A, Case B, and Case C,

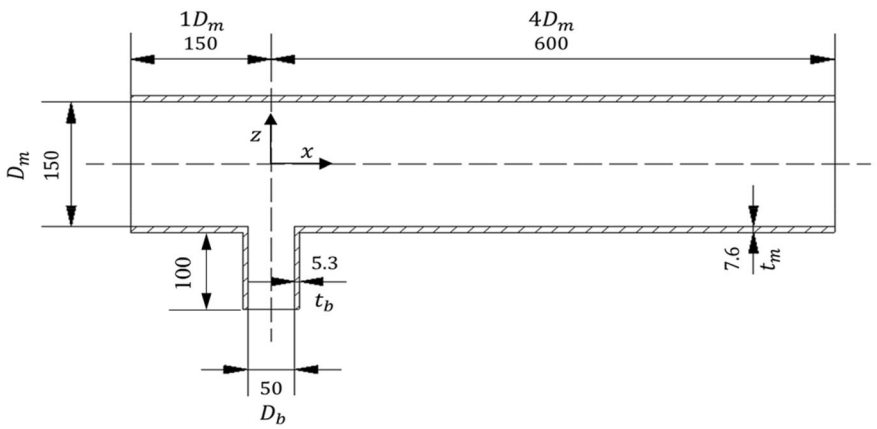

Fig. 1 Schematic diagram of simulated T pipe [mm]

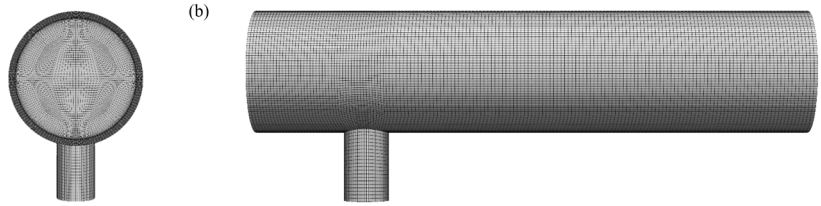

Fig. 2 View of the T junction pipe mesh from: **a** yz plane; **b** xz plane

respectively. Two more cases were considered to compare the FG pipe performance with that of the normal homogenous pipe. Case D with a structural steel pipe (homogenous) and Case E with two-layer structural steel-ceramic composite pipe reconsidered. The material properties of fluid and pipe components are tabulated in Table 2. Figure 3 depicts volume fraction of steel for each case along the non-dimensional thickness direction. A linear variation of the volume fraction was observed for a power-law index of 1. The fluid properties during the calculation were kept constant and obtained from the water properties at 40 °C.

ANSYS FLUENT (2019 R3) was used to perform the simulations. In order to obtain fully developed flow profile at the two inlets of the T junction pipe, another two pipes with the same diameter as the main and branch pipes were calculated with the identical inlet velocity presented in Table 1. The lengths of these two pipes are 10 D_m and 10 D_b, respectively. The velocity profiles at the outlets of the two pipes were mapped to the inlets of the T-junction pipe. The no-slip velocity boundary condition was used at the inner surface of pipe. For the thermal boundary condition, a coupled wall boundary condition was used at the interface of the fluid to the pipe and different layers interface within the pipe. The thermal boundary condition set outside the pipe was adiabatic.

Turbulence model selection is crucial for transient calculation. The Reynolds averaged Navier–Stokes (RANS) can be used for unsteady calculations because it can model the entire range of scales of turbulence, and it significantly reduces the computational effort

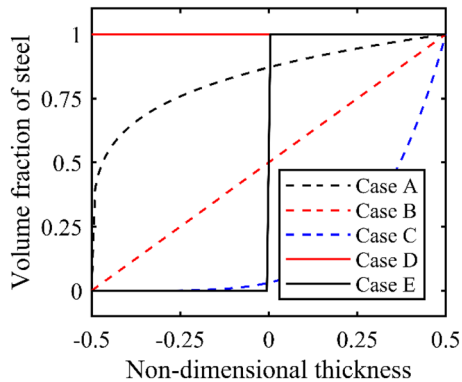

Fig. 3 Volume fraction of steel along the thickness

and resources. However, it is difficult to capture the fluctuation characteristics within the fluid in the RANS model; hence, it is not suitable for this study. Large eddy simulation (LES) in which small scales turbulence are spatially filtered out while large scales are resolved directly can also be used. Because the large scales of turbulence are resolved directly, the statistics of the time-varying RMS value can be collected; however, this requires a significant amount of computational resources. For pipe flow in particular, the resources needed in a near-wall resolving LES are unaffordable. Therefore, a hybrid RANS–LES model, that is, detached eddy simulation (DES), was adopted in this work. In DES, the RANS model is applied to the boundary layers, and LES is used in the other places. In the following simulation cases, the SST $k-\omega$ RANS model was used in the DES calculation.

Table 2 Material properties for thermal striping analysis

	Fluid	Structural steel	Ceramic
Density [kg/m^3]	992	7850	2300
Specific heat [J/(kg · K)]	4180	434	590
Thermal conductivity [W/(m · K)]	0.6	60.5	1.3
Viscosity [Pa · s]	$6.65 \cdot 10^{-6}$	–	–

Table 3 Turbulence model and numerical discretization

Software	ANSYS FLUENT 2019R3
Turbulence model	DES SST $k-\omega$
Pressure–velocity coupling	SIMPLE
Transient formulation	Bounded second order implicit
Momentum	Bounded central differencing
Energy	Second order upwind
Pressure	Second order
Turbulent kinetic energy	First order upwind
Specific dissipation rate	First order upwind

Table 3 presents the turbulence model and numerical discretization for the thermal striping simulation. The DES SST $k-\omega$ model require the y^+ value to be smaller than 1. With the $1.2\text{x}10^{-5}$ m thickness of the first layer, the maximum y^+ value during the calculation is 1.36. Although the maximum y^+ value is slightly larger than the required value 1, it occurred only on limited number of nodes. The time step was fixed as $2\text{x}10^{-4}$ s. Under this time step, iteration in each time step could converge within 20 times and the maximum Courant number is 0.82. Therefore, the Courant–Friedrichs–Lewy condition can also be satisfied. A total of 7 s physical time was obtained, and the last 5 s data were used for the statistical analysis.

2.3 Structural analysis of the T junction pipe

In the calculation presented in the previous section, a 7 s temperature field was obtained in the T-junction pipe under thermal striping. By importing this temperature field into the transient structural analysis module in ANSYS, the stress generated by thermal striping can be calculated.

The mesh used in the structural analysis is the same as that in the thermal striping simulation. There are a total of approximately 0.9 million nodes. The temperature field is saved every 100 time steps; therefore, the time step in the transient structural analysis is 0.02 s. The boundary condition of the pipe was set as free because the stress generated by the internal restraint is the primary concern. Five types of pipe cases (Cases A–E) were obtained as in the thermal striping simulation. Material properties for the structural simulation are tabulated in Table 4.

3 Results and discussion

3.1 Velocity field in fluid

The mean axial velocity at the central line on the $x = -0.36D_m$ cross-section before the T-junction mixing part is illustrated in Fig. 4a. The velocity profile from each case was compared with data from the WATLON experiment. It can be clearly observed that the mapped inlet velocity is sufficient to offer the fully developed flow profile before the mixing. It also indicates that before the flow passes the mixing part, the flow characteristics would not be affected by the different settings in the pipe through cases A–E.

Figure 4b presents the mean velocity at the downstream cross-section where $x = 1D_m$. There is a decrease in the magnitude of the mean axial velocity at the mixing part. A slight increase in the velocity at the upper part of the center was observed. This is because a recirculation zone is generated owing to mixing of the flow from the main and branch pipes. The recirculation zone is clearly recognized in Fig. 5a, which presents the mean velocity contour from Case D. Figure 5(b) shows the RMS value of the axial velocity calculated using Eq. (2) using the last 5 s of the data. It is easy to find the highest fluctuation occurring near the interface between the high-and low-velocity flows. The velocity contour also indicates that the wall jet flow of the thermal striping mainly influences the bottom part of the pipe.

$$u_{RMS} = \sqrt{\frac{\sum_{i=1}^{N}(u_i - u_{ave})^2}{N}} \tag{2}$$

In addition, in Fig. 4(b), the FGM cases, Case A-C which has 8 layers in the pipe domain, the velocity near the recirculation zone is smaller than WATLON data when compared with Case D and E. Because in Case D and Case E, the material in T junction pipe is completely different, the change in the composition of the T-junction pipe has minimal effect on the flow velocity. Therefore, the author infers the dividing pipe domain into 8 layers makes the difference between FGM cases and others. On the other hand, the good match of velocity RMS value between simulation and experiment verified that the used DES SST $k-\omega$ turbulence model can accurately capture the fluctuation characteristic in the flow caused by thermal striping. The low fluctuation intensity at the upper part

Table 4 Material properties for thermal stress analysis

	Structural steel	Ceramic
Density [kg/m^3]	7850	2300
Young's modulus [GPa]	200	90
Poisson's ratio	0.3	0.25
Coefficient of thermal expansion [/°C]	1.2x10^{-5}	1.4x10^{-6}

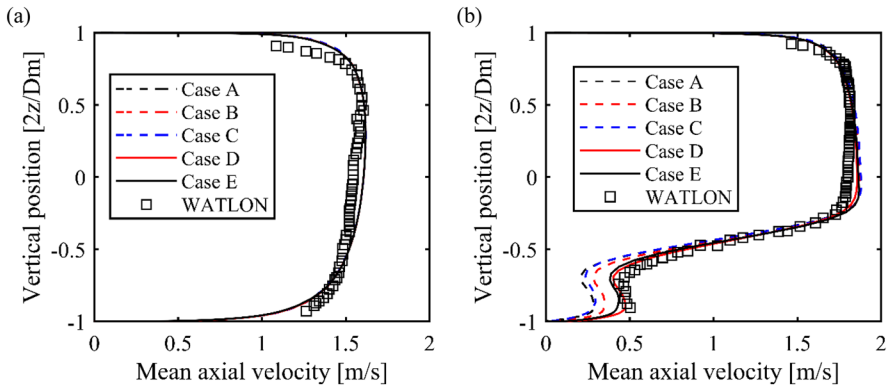

Fig. 4 Mean axial velocity profile of the central line at: **a** $x = -0.36D_m$, **b** $x = 1D_m$

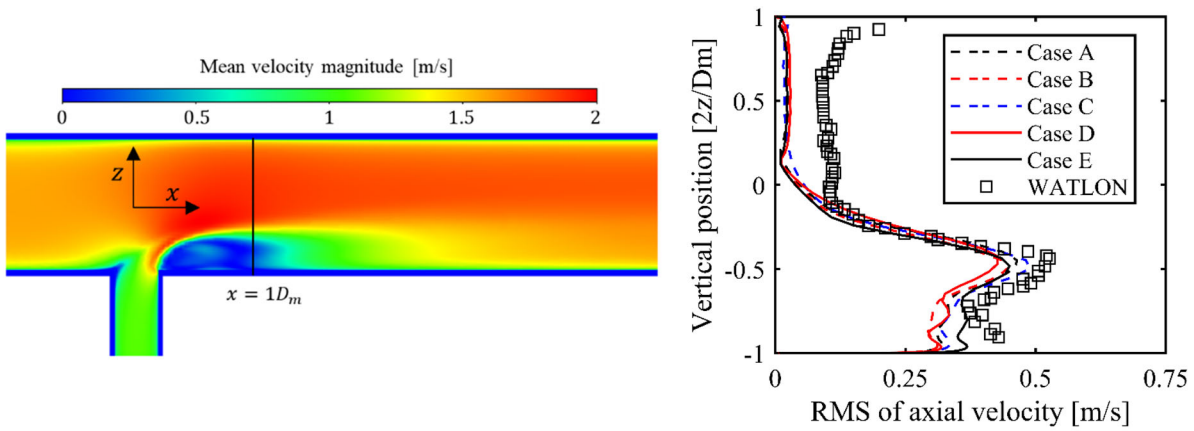

Fig. 5 **a** Mean velocity contour at YZ plane from Case D, **b** RMS of axial velocity at the central line at $x = 1D_m$

of the flow is considered to be near wall flow and was treated using the RANS model SST $k - \omega$.

3.2 Temperature fluctuation

The temperature fluctuation caused by thermal striping is the primary focus of this study. Figure 6 shows the mean static temperature contour at the $x = 1D_m$ cross-section for each case. In the homogenous steel pipe (Case D) and ceramic steel two-layer composite pipe (Case E), the separation of the temperature field between inner ceramic layer and outer steel layer could be clearly observed from Case E. The existence of a thermally resistant ceramic prevents temperature transfer to the outer steel layer to some degree. However, it also causes an uneven temperature profile in the T-junction pipe along thickness direction. The three FG cases showed similar mean temperature distributions in the fluid domain. The low-temperature region is limited to the bottom part of the pipe, which is a characteristic of wall jet flow. In the solid domain, the ceramic-rich Case C, which has a power law index

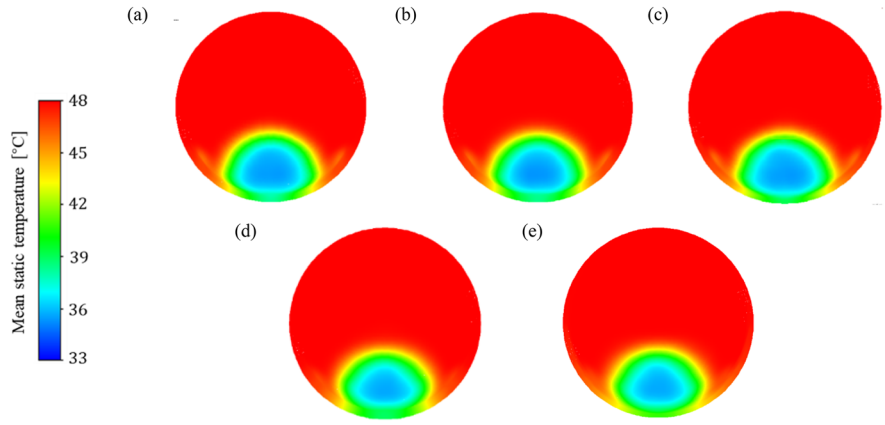

Fig. 6 Mean temperature contours at the x = 1D_m XY plane for each case

of N = 5, also has a slight temperature separation near the outer part of the pipe, similar to Case E.

A schematic diagram of different positions used for statistical analysis is shown in Fig. 7. In the fluid domain, the temperature fluctuation on a curve of 1 mm from the interface of the fluid and pipe was also calculated, in addition to the vertical central line of the cross-section. Then, power spectral density of temperature was calculated on three points in the 0°, 30°, and 60° directions. In the solid domain, the temperature fluctuations on three curves, the inner wall of the pipe, 1 mm to the inner wall, and 1 mm to the outer wall were determined. For the temperature power spectral density in the solid, points in the 30° direction were used. To compare with data from the WATLON experiment, we used the non-dimensional temperature

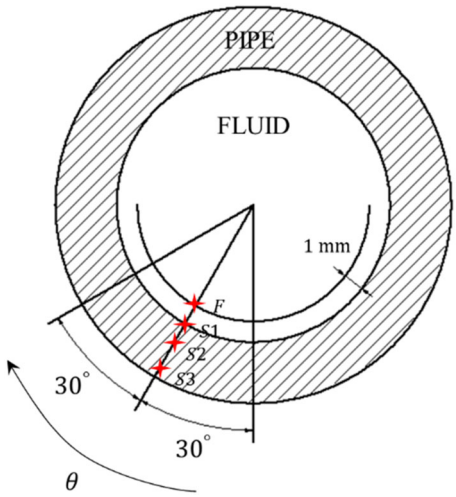

Fig. 7 Schematic diagram of the $x = 1D_m$ cross-section

T^*. The definition of T^* and RMS calculation is described in Eq. (3).

$$T^* = \frac{T - T_b}{T_m - T_b}, T^*_{RMS} = \sqrt{\frac{\sum_{i=1}^{N} \left(T^*_i - T^*_{ave}\right)^2}{N}} \quad (3)$$

The mean non-dimensional temperature and temperature fluctuation in the central line and the curve near the pipe in the fluid domain are shown in Fig. 8. The bottom part of the pipe shows a higher fluctuation in temperature intensity owing to mixing of the two flows. The peak value was observed in the region where the high-and low-temperature fluid separated. The temperature profiles from cases A to E are similar, indicating that differences in pipe material do not affect the flow characteristics. Although there is a difference in non-dimensional mean temperature between simulation cases and WATLON, a close match in the temperature RMS value, which is more crucial in terms of evaluating thermal striping, confirms the feasibility of the mesh and turbulence model used in the simulation. The mean non-dimensional temperature and fluctuation intensity at the curve near the interface are presented in Fig. 8c and d, respectively. After 90°, temperature has the same value as that in the main pipe, and the fluctuations also disappear. Combining the temperature profiles on the central line, it can be observed that in the wall jet flow of thermal striping, the bottom half of the flow is mainly affected. The peak of the temperature fluctuation in the region close to the interface will occur in the 30° direction.

Figure 9 depicts the temperature profiles of the three curves within pipe. From left to right, the figure shows the curves at the pipe wall, 1 mm to the

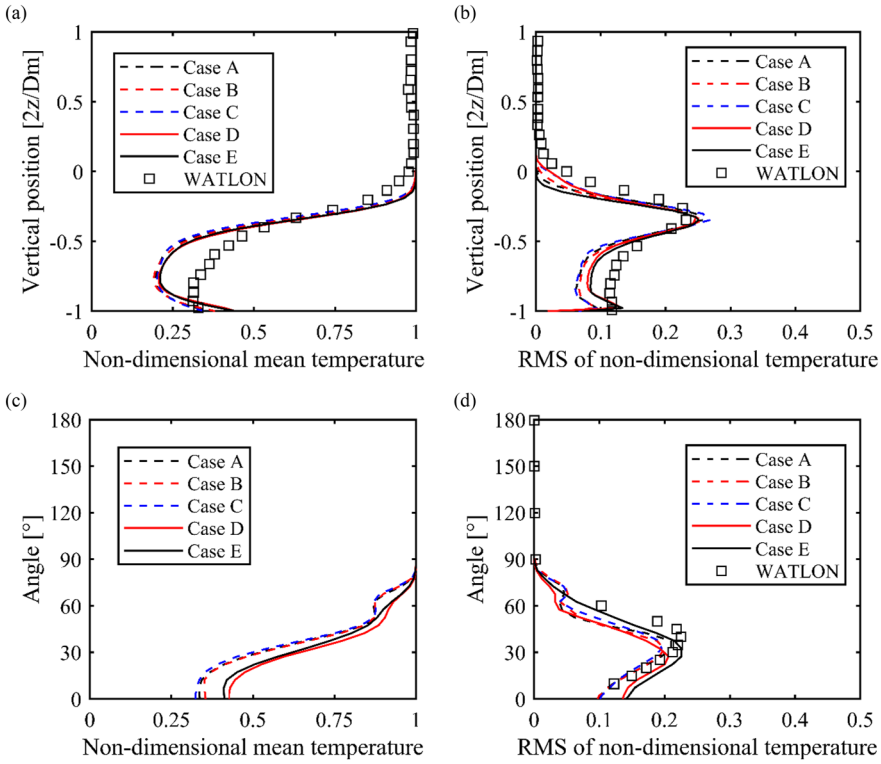

Fig. 8 Temperature field in the fluid at $x = 1D_m$: **a** mean non-dimensional temperature and **b** fluctuation intensity at the central line; **c** mean non-dimensional temperature and **d** fluctuation intensity at the curve near the pipe

inner wall, and 1 mm to the outer wall. It can be observed that the low-temperature region becomes smaller when the distance increases gradually away from the fluid. In curves near the outer wall in Fig. 9c, Cases C and E have a relatively smooth temperature change on the curves, which shows that a high ratio in the ceramic volume fraction could relieve the sharp change in the temperature distribution. In the temperature fluctuation intensity plots, only the curves at the pipe wall retain the peak fluctuation value at 30°, as in the fluid domain. However, the fluctuation intensity is much smaller than that in the fluid domain. The fluctuations in the temperature are almost negligible in the curves near the outer wall. Although different compositions in the pipe can result in a difference in the mean temperature distribution in the pipe, however, in terms of temperature fluctuation, both cases provide a similar result.

In addition to statistical analysis of the temperature field, spectral analysis of the last 5 s data in each case was performed to determine the frequencies in the fluctuations caused by the thermal striping. Figure 10 shows the power spectral density of the three points on the curve in the fluid at a distance of 1 mm from the pipe. It can be observed that the fluctuation power in the fluid domain is almost the same in both cases. In the 30° and 60° direction points, the 6 Hz component contains the peak fluctuation power, which is also consistent with the result obtained by Evrim and Laurien (2020) using large eddy simulation and as well as the WATLON experiment data. In the 0°direction, the peak fluctuation power is on the 13 Hz component. However, similar to the RMS value in Fig. 8d, the 30° points have the largest fluctuation power. Therefore, in the solid domain, the temperature PSD of four points in the 30° direction from each case was calculated. The PSD of the temperature in the solid domain is shown in Fig. 11. In each case, the PSD plot in the solid shows that the temperature fluctuation decreases as the distance between the points and fluid gradually increases. This clearly indicates that in the PSD of Point S2, which is on the curve 1 mm to the inner wall, the characteristic of the 6 Hz component has a peak fluctuation power. However, at Point S3, which is close to the outer wall, no peak frequency was observed. In the PSD of Cases C and E, the fluctuation from Point S3 cannot be

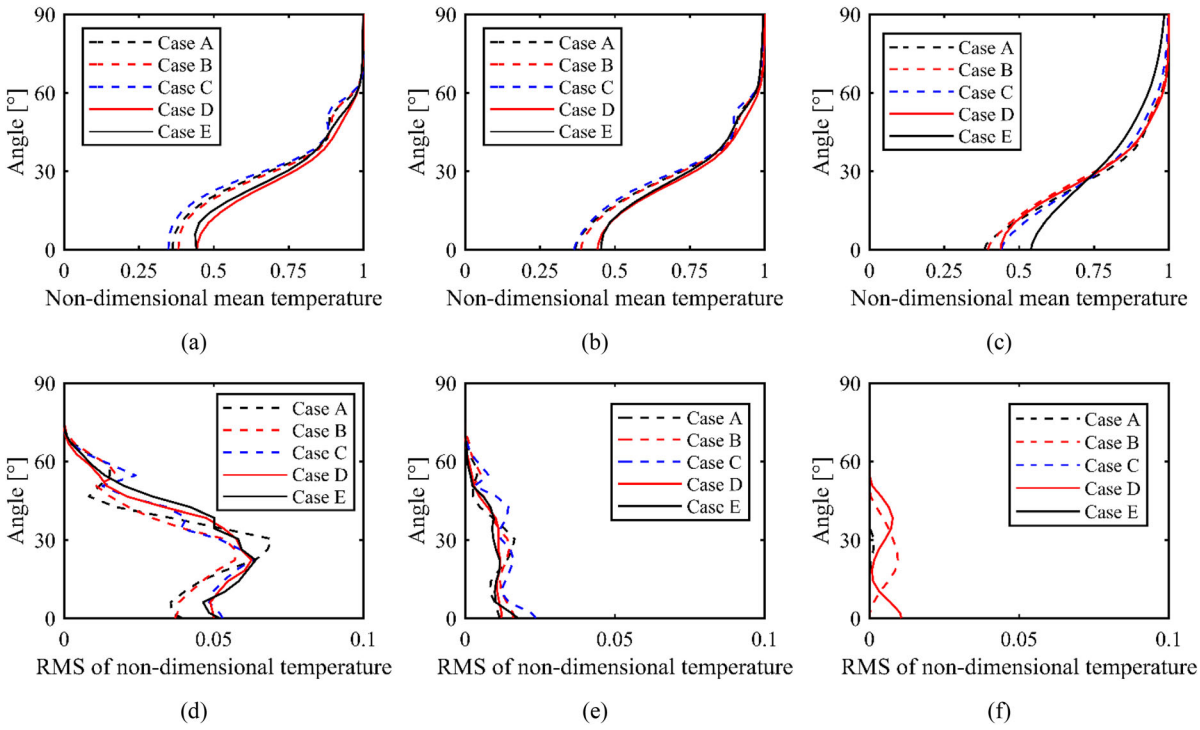

Fig. 9 Temperature field in the solid at $x = 1D_m$: **a** mean non-dimensional temperature and **d** temperature RMS at the pipe wall; **b** mean non-dimensional temperature and **e** temperature RMS at the curve 1 mm to the inner wall; **c** mean non-dimensional temperature and **f** temperature RMS at the curve 1 mm to the outer wall

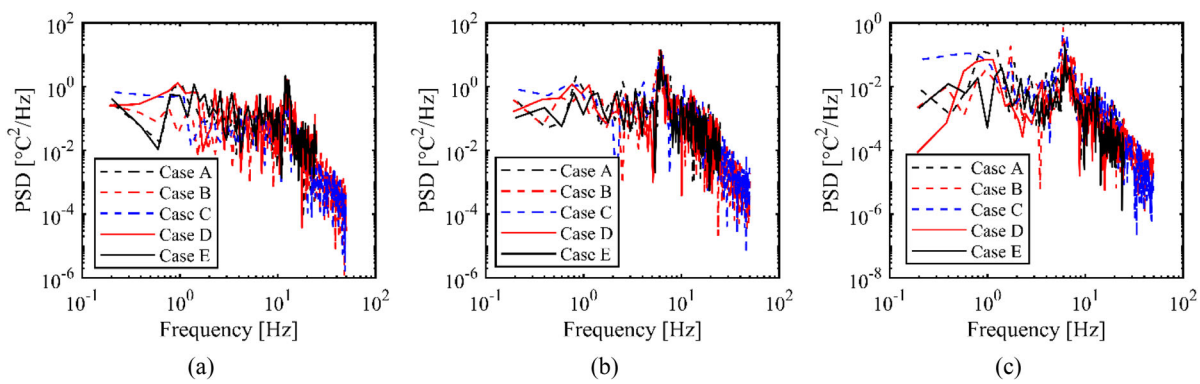

Fig. 10 Temperature PSD of the points in the fluid on the curve near the wall: **a** 0°; **b** 30°; **c** 60°

captured as a large volume fraction of ceramic is present.

3.3 Thermal stress in T pipe

Transient structural analysis was performed for each case of the T-junction pipe by importing the temperature history in the pipe domain from the thermal striping simulation. Similar to the analysis of the temperature field in the pipe, the PSD of the stress at the points at 30° was calculated. Figure 12 shows the stress PSD results. It can be observed that when the volume fraction of the ceramic is increased in the pipe, the power of the stress fluctuation gradually decreases from Case A to Case C and in Case E. It should be pointed out that for the two-layer composite pipe

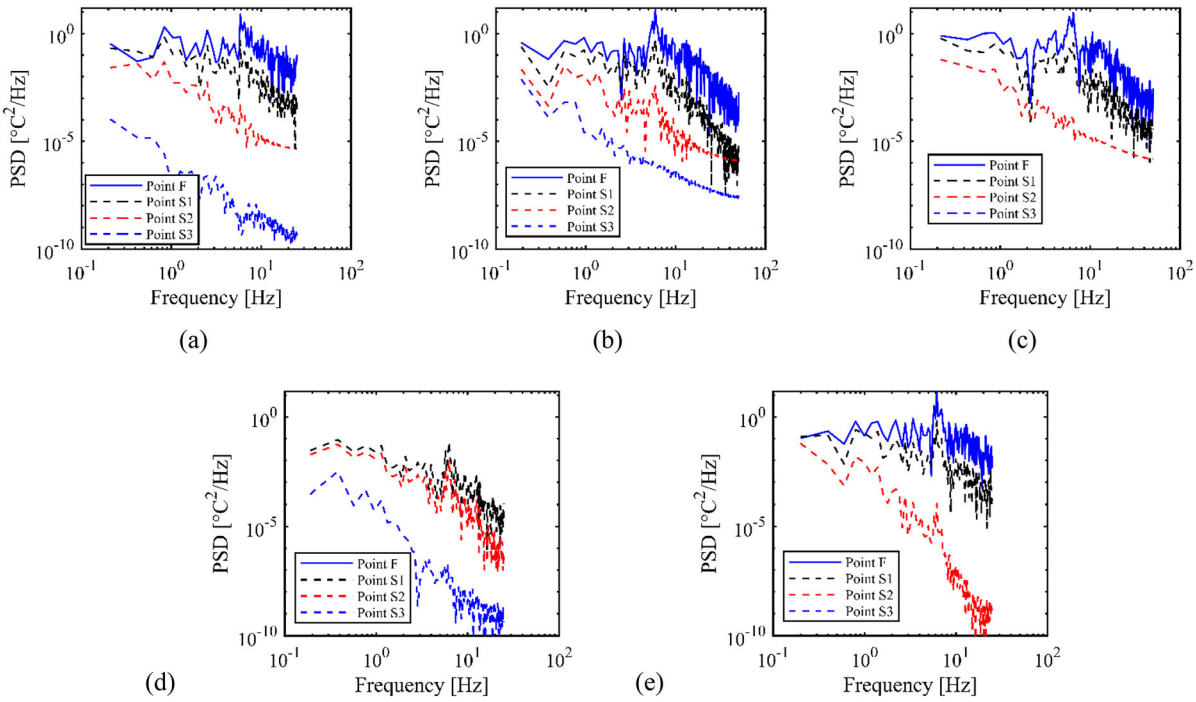

Fig. 11 Temperature power spectral density of the points in the solid at 60° direction: **a** Case A; **b** Case B; **c** Case C; **d** Case D; **e** Case E

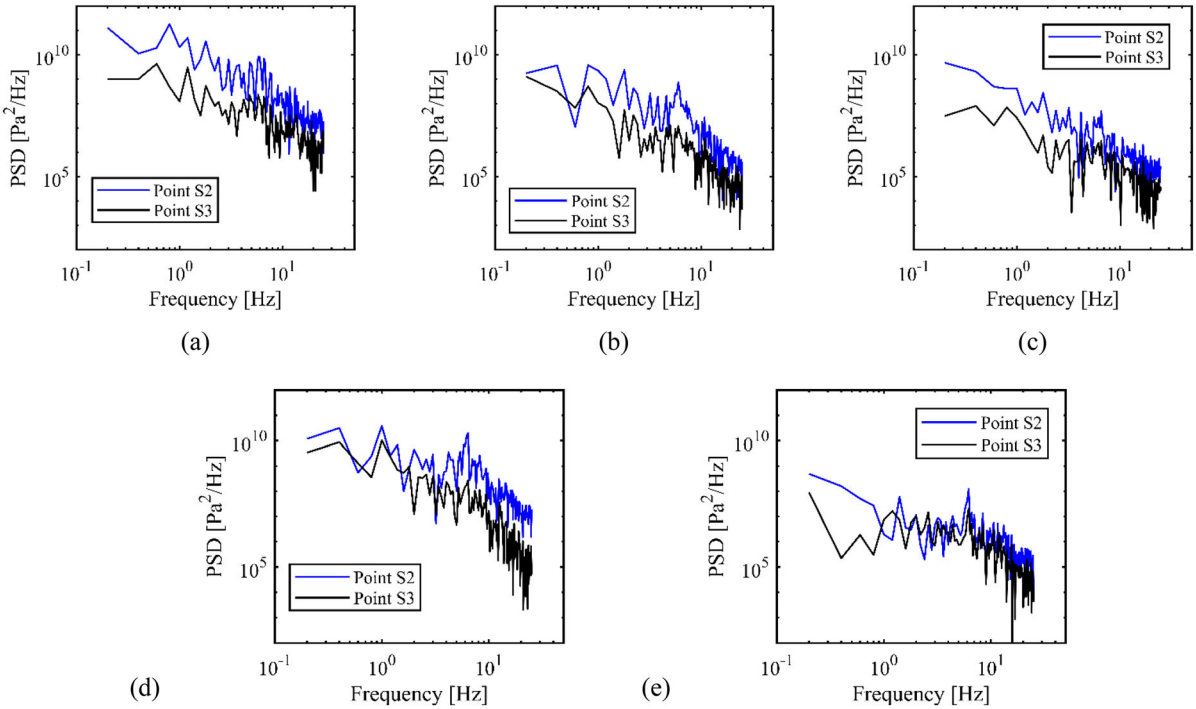

Fig. 12 Stress power spectral density of the points in the solid at 60° direction: **a** Case A; **b** Case B; **c** Case C; **d** Case D; **e** Case E

(Case E), the same fluctuation is observed for points near the outer and inner walls. In the homogenous pipe (Case D), the fluctuation in the position close to the outer surface is smaller than that near inner surface. The FG pipes (Cases A–C) exhibit similar behavior to the homogenous case. In the stress PSD, the peak power occurred at 6 Hz, which is the same as the temperature fluctuation. They differ only at the point near the outer wall where fluctuation in the temperature has already ceased; the 6 Hz frequency component retains the largest stress fluctuation power.

In addition to spectral analysis, the rainflow counting method was used on the stress history to capture the stress cycle generated in the pipe due to thermal striping. Table 5 lists the stress cycle mean amplitude and average stress at points S2 and S3. From the average stress, it can be observed that the homogenous steel pipe (Case D) has the lowest average stress. However, the average stresses in the other cases with ceramic are larger. This can be attributed to the fact that the homogenous pipe has a relatively average temperature distribution in the thickness direction. The other configuration with two-layer composite pipe (Case E) has a different temperature distribution, as shown in Fig. 6(e). This specific variation in the temperature field may lead to uneven deformation due to thermal expansion and finally lead to high stress generation. However, the homogenous steel pipe has the largest amplitude in the mean amplitude of the stress cycle. This is because without the thermal resistant ceramic, the temperature fluctuation generated from the thermal striping directly affects the stress fluctuation within the pipe. In FG T pipe cases, the mean stress lies between the homogenous steel pipe and the two-layer composite pipe. The mean amplitude gradually decreases with an increase in the ceramic volume fraction as it can be seen in the Table 5 from Case A to Case C. It shows the FGM has the ability to reduce the amplitude of the stress cycle generated by the thermal striping while mean stress level can be monitored and tailor-made based on specific need. Highest amplitude is observed for the homogeneous (Case D) configuration while two-layer composite (Case E) predicts lower amplitude. Use of FGM with power law index 5 will reduce the amplitude ratio close to homogeneous structure while it will reduce the thermal stripping significantly. Therefore, it can be concluded that use of FGM with higher ceramic volume fraction (governed by power law index, N = 5) can be used in T junction pipe to reduce the thermal stripping and increase the fatigue life of the component.

Further, in order to estimate the fatigue life for each case T junction pipe, a fatigue safety factor based on the Gerber method was applied. Equation 4 gives the way to estimate the fatigue safety factor by the stress amplitude and mean stress from the stress cycle.

$$\frac{1}{SF} = max\left(\frac{(\sigma_A)_i}{S_f} + \left(\frac{(\sigma_M)_i}{S_u}\right)^2\right) \tag{4}$$

where S_f is fatigue limit and S_u is the ultimate strength.

Based on Eq. 4, the parameter $\eta = \sum_i (\frac{(\sigma_A)_i}{S_f} + \left(\frac{(\sigma_M)_i}{S_u}\right)^2)/i$ which represents the average stress cycle risk was calculated for each case and listed in Table 6. Because the low-temperature difference, only 15 °C in the simulation, the value of η from each case is small. However, for the functionally graded T pipe, Case A to C, the clearly decrease trend in the η could be

Table 5 Mean amplitude and mean stress of the stress cycle at points S2 and S3

	Point S2 [MPa]			Point S3 [MPa]		
	Mean amplitude [MPa]	Average stress [MPa]	A/M (%)	Mean amplitude [kPa]	Average stress [MPa]	A/M (%)
Case A	0.33	10.35	32.1	54.6	10.35	5.3
Case B	0.08	14.07	5.5	13.9	17.28	0.8
Case C	0.02	6.72	2.9	7.3	13.55	0.5
Case D	0.32	1.60	199.4	75.6	1.29	58.9
Case E	0.02	20.40	1.1	9.3	20.48	0.5

Table 6 Fatigue safety factor from each case

	Case A	Case B	Case C	Case D	Case E
η	0.0022	0.0013	0.0003	0.0017	0.0019

observed. The power law index N in these 3 cases are 0.2, 1, and 5, respectively. This means the composition of ceramic is gradually increase. The present result shows by applying FGM to the T junction pipe, the performance in terms of resisting thermal fatigue generated by thermal striping could be improved.

4 Conclusions

A numerical study on the behavior of a T pipe made of FGM under thermal striping was conducted using the detached eddy simulation (DES) method. Temperature data of T junction pipe was obtained from the thermal stripping simulation through statistical and spectral analyses; furthermore, the transient stress was determined. The results of the present analysis were compared with data from the WATLON experiment. The similarities in the RMS value from the two studies indicate that the present DES SST $k - \omega$ turbulence model can accurately capture the temperature fluctuation in the thermal striping. However, the differences in the mean velocity field and temperature field indicate the limitation of DES turbulence model and FGM modeling method. The following conclusions can be drawn from the results of the present study:

1. The mean temperature distribution in the composite pipe exhibited a separation phenomenon, whereas the FG pipe cases have a more even distribution like the homogenous pipe.
2. The 6 Hz component in the temperature fluctuation caused by thermal striping has the largest fluctuation power, and the 30° direction in the pipe has the highest fluctuation intensity.
3. The 6 Hz peak power frequency is maintained when the temperature is transferred from the fluid to the pipe wall. However, this peak frequency component disappears at the outer side of the pipe. On the other hand, the stress generated throughout the pipe maintains optimal power on the 6 Hz component, unlike the temperature.
4. The mean stress in the homogenous pipe generated by thermal striping is smaller than that in the composite and FG pipes owing to the even distribution of temperature across the thickness. However, the stress cycle amplitude is much larger.
5. FG pipe experiences lower stress amplitude as a result thermal stripping phenomenon will be reduced.

Acknowledgements The authors gratefully acknowledge the financial supports of this research by the Grant-in-Aid for Scientific Research (C) of the Ministry of Education, Culture, Sports, Science and Technology, Japan (MEXT Grant) [Grant No. 19K04087]. The authors declare no conflict of interest in preparing this article.

Authors' contributions All authors contributed to the study conception and design. The first draft of the manuscript was written by Ziyi Su and all authors commented on previous versions of the manuscript. All authors read and approved the final manuscript.

Funding The authors gratefully acknowledge the financial supports of this research by the Grant-in-Aid for Scientific Research (C) of the Ministry of Education, Culture, Sports, Science and Technology, Japan (MEXT Grant) [Grant No. 19K04087].

Data availability The data that support the findings of this study are available from the corresponding author, Ziyi Su, upon reasonable request.

Declarations

Conflict of interest The authors declare no conflict of interest in preparing this article.

References

Ayhan, H., Sökmen, C.N.: CFD modeling of thermal mixing in a T-junction geometry using LES model. Nucl. Eng. Des. **253**, 183–191 (2012)

Blondet, E., Faidy, C.: High cycle thermal fatigue in French PWR. In International Conference on Nuclear Engineering **35952**, 429–436 (2002)

Chadeyron, P.: Communication report regarding the incident on the residual heat removal system at the nuclear power plant of Civaux May 12, 1998 (1999)

Chapuliot, S., Gourdin, C., Payen, T., Magnaud, J.P., Monavon, A.: Hydro-thermal-mechanical analysis of thermal fatigue in a mixing tee. Nucl. Eng. Des. **235**(5), 575–596 (2005)

Chuang, G.Y., Ferng, Y.M.: Experimentally investigating the thermal mixing and thermal stripping characteristics in a T-junction. Appl. Therm. Eng. **113**, 1585–1595 (2017)

Das, A., Karmakar, A.: Free vibration characteristics of functionally graded pre-twisted conical shells under rotation. J.Inst. Eng. (India): Series C, 99(6), 681–692 (2018)

Evrim, C., Laurien, E.: Large-Eddy Simulation of turbulent thermal flow mixing in a vertical T-Junction configuration. Int. J. Thermal Sci. **150**, 106231 (2020)

Evrim, C., Laurien, E.: Numerical study of thermal mixing mechanisms in t-junctions. Appl. Thermal Eng. **183**, 116155 (2021)

Höhne, T.: Scale resolved simulations of the OECD/NEA–Vattenfall T-junction benchmark. Nucl. Eng. Des. **269**, 149–154 (2014)

Jayaraju, S.T., Komen, E.M.J., Baglietto, E.: Suitability of wall-functions in Large Eddy Simulation for thermal fatigue in a T-junction. Nucl. Eng. Des. **240**(10), 2544–2554 (2010)

Kamide, H., Igarashi, M., Kawashima, S., Kimura, N., Hayashi, K.: Study on mixing behavior in a tee piping and numerical analyses for evaluation of thermal striping. Nucl. Eng. Des. **239**(1), 58–67 (2009)

Kang, D.G., Na, H., Lee, C.Y.: Detached eddy simulation of turbulent and thermal mixing in a T-junction. Ann. Nucl. Energy **124**, 245–256 (2019)

Kawamura, T., Shiina, K., Ohtsuka, M.: Thermal striping tests in mixing tees with same pipe diameters. 1st report, characteristics of flow patterns and fluid temperature fluctuations. Nippon Kikai Gakkai Ronbunshu, B Hen, 69(682), 1445–1452 (2003)

Kawasaki, A., Watanabe, R.: Concept and P/M fabrication of functionally gradient materials. Ceram. Int. **23**(1), 73–83 (1997)

Miyoshi, K., Nakamura, A., Utanohara, Y.: An investigation of wall temperature characteristics to improve evaluation method for thermal fatigue at a T-junction pipe. INSS Journal **20**, 45–55 (2013)

Nakamura, A., Oumaya, T., Takenaka, N.: Numerical investigation of thermal striping at a mixing tee using detached eddy simulation. (2009)

Nakamura, A.: Numerical simulations of thermal striping at T-junction pipe. The effect of turbulence model and computational grid. INSS Journal, 14, 99–115 (2007)

Saleh, B., Jiang, J., Fathi, R., Al-hababi, T., Xu, Q., Wang, L., ... Ma, A.: 30 Years of functionally graded materials: An overview of manufacturing methods, Applications and Future Challenges. Composites Part B: Engineering, 108376 (2020)

Selvam, P.K., Kulenovic, R., Laurien, E.: Large eddy simulation on thermal mixing of fluids in a T-junction with conjugate heat transfer. Nucl. Eng. Des. **284**, 238–246 (2015)

Su Z., Inaba K., Karmakar A., Das A.: Analytical and numerical study of vibration and transient heat conduction in a functionally graded pipe. Journal of Advanced Mechanical Design, Systems, and Manufacturing, 15(5), JAMDSM0054-JAMDSM0054 (2021)

Tanaka, M., Ohshima, H., Monji, H.: Thermal mixing in T-junction piping system related to high-cycle thermal fatigue in structure. J. Nucl. Sci. Technol. **47**(9), 790–801 (2010)

Timperi, A.: Conjugate heat transfer LES of thermal mixing in a T-junction. Nucl. Eng. Des. **273**, 483–496 (2014)

Watanabe, Y., Kim, I.S., Fukui, Y.: Microstructures of functionally graded materials fabricated by centrifugal solid-particle and in-situ methods. Met. Mater. Int. **11**(5), 391–399 (2005)

Zhou, M., Kulenovic, R., Laurien, E.: Advanced flow pattern for describing tangential flow oscillation in thermal-mixing pipe flow at a horizontal T-Junction. Int. J. Therm. Sci. **136**, 328–336 (2019a)

Zhou, M., Kulenovic, R., Laurien, E.: T-junction experiments to investigate thermal-mixing pipe flow with combined measurement techniques. Appl. Therm. Eng. **150**, 237–249 (2019b)